Out-of-Cycle Update

of the US/UK World Magnetic Model

for 2015-2020

Arnaud Chulliat
   Patrick Alken
   Manoj Nair
   Adam Woods
   Brian Meyer
   Robert Redmon

William Brown
   Susan Macmillan
   Ciaran Beggan
   Brian Hamilton

NOAA National Centers for
Environmental Information
325 Broadway
NOAA E/NE42
Boulder, CO 80305
USA

British Geological Survey
Geomagnetism Team
The Lyell Centre
Research Avenue South
Edinburgh EH14 4AP
UK

Abstract

*In early 2018, the World Magnetic Model 2015-2020 (WMM2015) was predicted to exceed its performance specification error tolerances by the end of 2018 or early 2019. Specifically, the grid variation root-mean-square error was about to exceed the 1 degree specification (MIL-PRF-89500A) due to fast fluid flows in the Earth's outer core, especially in the North polar region. An out-of-cycle update of the WMM2015 was developed and released in early 2019 (*WMM2015v2) *to address this performance degradation. There was a pre-release in September 2018 and this technical note confirms the information provided in that pre-release. It also provides a description of the new model (section 1), how it was produced (section 2) and its uncertainties (section 3).*

How to Use this Note: A complete description of the WMM2015 is provided in the WMM2015 Technical Report (Chulliat *et al.*, 2015; WMM2015-TR hereafter). This new technical note should be seen as an addendum to the WMM2015-TR. It is organized in the same manner as the WMM2015-TR in order to facilitate the retrieval of information by users. It only includes information that is new for the out-of-cycle update, hereafter referred to as WMM2015v2.

1. The Model

The following subsections in the WMM2015-TR are updated below: 1.3, 1.4, 1.6, 1.8, and 1.10. All other sections are still applicable. In particular, the model equations and validity range (2015-2020) are unchanged. Subsection 1.5 (high-precision numerical example) remains applicable provided one uses the WMM2015.

a. WMM2015v2 Coefficients (§1.3 in the WMM2015-TR)

The updated (WMM2015v2) coefficient file is available from

- https://www.ngdc.noaa.gov/geomag/WMM/,
- http://www.geomag.bgs.ac.uk/research/modelling/WorldMagneticModel.html and
- http://earth-info.nga.mil/GandG/update/index.php?action=home.

It has the same name (WMM.COF) as the WMM2015 coefficient file. However, the header is different and reads:

```
2015.0              WMM-2015v2      09/18/2018
```

For many users, replacing the old coefficient file with the new one is the only step required to update the WMM software to WMM2015v2.

b. Singularities at the Geographic Poles (§1.4 in the WMM2015-TR)

When using the new model, the third paragraph in the WMM2015-TR, subsection 1.4 should read: "On 1 January 2019, directly above the North (resp. South) Pole at 6,371,200 meters from the Earth's center, the magnetic field vector lies in the half-plane of the 178.72°E (resp. 30.67°W) meridian. If the Pole is assigned $\lambda = 0^°$, the components X', Y', Z' (also the components X, Y, Z) are 1826.6 nT, 40.9 nT, and 56362.8 nT respectively at the North Pole, 14287.5 nT, -8473.9 nT and -51734.0 nT respectively at the South Pole. A change in the longitude assigned to the Pole is equivalent to a rotation of the NED frame about the polar axis." (Note: in the WMM2015-TR, the value provided for the half-plane meridian containing the magnetic field vector at the South Pole was erroneous; it should read 30.14°W.)

c. Supersession of the Models (§1.6 in the WMM2015-TR)

WMM2015v2 supersedes WMM2015 and should replace it in navigation and other systems. Unlike WMM2015, WMM2015v2 is expected to meet the WMM performance specification from January 1, 2015 to December 31, 2019 (see section 3). *However, noting that the WMM2015 performance degradation issue only affects*

locations in the Arctic region, it is still acceptable to rely on WMM2015 in systems not used above 55 degrees latitude in the Northern hemisphere.

In late December 2019, barring unforeseen circumstances, the U.S. and U.K. agencies will replace WMM2015v2 with WMM2020, a new degree and order 12 main field and secular-variation model valid from January 1, 2020 to December 31, 2024.

d. Magnetic Poles and Geomagnetic Coordinate Systems (§1.8 in the WMM2015-TR)

The pole locations and magnetic field values provided in the WMM2015-TR, subsection 1.8 (both in the main text and in Table 4) are updated using WMM2015v2 in Table 1.

Table 1: Computed pole positions based on the WMM2015v2.

	Date	North	South
Geomagnetic Poles	2019.0	72.69° W 80.55° N (geocentric) 80.61° N (geodetic)	107.31° E 80.55° S (geocentric) 80.61° S (geodetic)
Model Dip Poles	2019.0	170.88° E 86.54° N	136.02° E 64.13° S
Eccentric Dipole	2019.0	r = 588 km; φ' = 22.66°N; λ = 137.35°E	

e. Test Values (§1.10 in the WMM2015-TR)

The test values provided in the WMM2015-TR, subsection 1.10 (Table 5) are updated using WMM2015v2 in Table 2. Note that the same dates and locations are used.

Table 2: Test values for WMM2015v2. The computation was carried out with double precision arithmetic. Single precision arithmetic can cause differences of up to 0.1 nT. Heights are with respect to the WGS 84 ellipsoid. Grid Variation is with respect to the Grid North of the Universal Polar Stereographic Projection.

Date	Height (km)	Lat (Deg)	Lon (Deg)	X (nT)	Y (nT)	Z (nT)	H (nT)	F (nT)	I (Deg)	D (Deg)	GV (Deg)
2015	0	80	0	6636.6	-451.9	54408.9	6651.9	54814.0	83.03	-3.90	-3.90
2015	0	0	120	39521.1	377.7	-11228.8	39522.9	41087.1	-15.86	0.55	0.55
2015	0	-80	240	5796.3	15759.1	-52927.1	16791.2	55526.8	-72.40	69.81	309.81
2015	100	80	0	6323.4	-477.6	52249.1	6341.4	52632.5	83.08	-4.32	-4.32
2015	100	0	120	37538.1	351.1	-10751.1	37539.7	39048.9	-15.98	0.54	0.54
2015	100	-80	240	5612.2	14789.3	-50385.8	15818.3	52810.5	-72.57	69.22	309.22
2017.5	0	80	0	6605.2	-298.7	54506.3	6612.0	54905.9	83.08	-2.59	-2.59
2017.5	0	0	120	39569.4	252.3	-11067.9	39570.2	41088.9	-15.63	0.37	0.37
2017.5	0	-80	240	5864.6	15764.1	-52706.1	16819.7	55324.8	-72.30	69.59	309.59
2017.5	100	80	0	6294.3	-331.1	52337.8	6303.0	52716.0	83.13	-3.01	-3.01
2017.5	100	0	120	37584.4	235.7	-10600.5	37585.1	39051.4	-15.75	0.36	0.36
2017.5	100	-80	240	5674.9	14793.1	-50179.5	15844.2	52621.5	-72.48	69.01	309.01

Date	Height (km)	Lat (Deg)	Lon (Deg)	Xdot (nT/yr)	Ydot (nT/yr)	Zdot (nT/yr)	Hdot (nT/yr)	Fdot (nT/yr)	Idot (Deg/yr)	Ddot (Deg/yr)
2015	0	80	0	-12.6	61.3	39.0	-16.7	36.7	0.02	0.52
2015	0	0	120	19.3	-50.2	64.3	18.8	0.5	0.09	-0.07
2015	0	-80	240	27.3	2.0	88.4	11.3	-80.8	0.04	-0.09
2015	100	80	0	-11.6	58.6	35.5	-16.0	33.3	0.02	0.52
2015	100	0	120	18.5	-46.1	60.2	18.1	0.8	0.09	-0.07
2015	100	-80	240	25.1	1.5	82.5	10.3	-75.6	0.04	-0.08
2017.5	0	80	0	-12.6	61.3	39.0	-15.3	36.9	0.02	0.53
2017.5	0	0	120	19.3	-50.2	64.3	19.0	1.0	0.09	-0.07
2017.5	0	-80	240	27.3	2.0	88.4	11.4	-80.7	0.04	-0.08
2017.5	100	80	0	-11.6	58.6	35.5	-14.7	33.5	0.02	0.53
2017.5	100	0	120	18.5	-46.1	60.2	18.2	1.2	0.09	-0.07
2017.5	100	-80	240	25.1	1.5	82.5	10.4	-75.6	0.04	-0.08

2. Construction of the Model

The information provided in subsections 2.1 ("Background on the geomagnetic field") and 2.2 ("Data acquisition and quality control") of the WMM2015-TR is still applicable. However, the description of how the model was derived needs to be updated, as more recent data were used and the modeling methodology has evolved since 2014. The general approach is the same, but different data selection criteria, corrections, weighting and inversion parameters were used.

As with the WMM2015, parent models were developed, which include the spherical harmonic degree and order 12 core field coefficients represented by WMM, but also include extended parameters to represent other aspects of the geomagnetic field as well as satellite attitude information. For this WMM2015v2 out-of-cycle update, two parent models were developed, one by the team at NOAA/NCEI and the other by the team at BGS. These two parent models were then combined into the final WMM2015v2. Details of these parent models and the methodology used in combining them is described below.

a. NOAA/NCEI Parent Model

i. Data selection

Magnetic field measurements from the Swarm A and B satellites were used, spanning the three year time interval 2015.52 to 2018.52, and subsampled to 30 seconds, corresponding to about 210-km along-track spacing. Vector measurements were used at mid and low-latitudes (between -55° and +55° geomagnetic latitude), while scalar field data was used at all latitudes. In the mid/low-latitude region, data were selected from the 00:00 to 05:00 local time sector. At high-latitudes (above 55° geomagnetic latitude), data with a solar zenith angle less than 100° were excluded to ensure the satellites are in darkness.

The following criteria were applied to the satellite measurement timestamps to select data during geomagnetically quiet periods:

- Kp <= 2o
- |dRC/dt| <= 3 nT/hour

Here, RC is an index designed to track the strength of the magnetospheric ring current. It is similar to the Dst index but calculated from a larger number of mid and low-latitude ground observatories (Olsen *et al.,*2014). The Kp index is described in the WMM2015-TR.

ii. Data correction and weighting

- The external magnetospheric model developed by Lühr and Maus, 2010 was subtracted from the Swarm measurements to minimize known variations from currents in the magnetosphere.

- For Swarm vector measurements, Euler angles were co-estimated with the internal Gauss coefficients, which represent a fixed rotation from the fluxgate magnetometer instrument frame to the star camera frame.
- The local data density per unit area at orbital altitude was determined and used to spatially weight the data, in order to ensure an equal weighting in the model from each region of the globe.

iii. Model description

The parent model is comprised of:

- The static part of the internal field to spherical harmonic degree and order 35
- The secular variation (SV) to degree and order 15
- The secular acceleration (SA) to degree and order 10

The Gauss coefficients were parameterized by a 2nd order Taylor series expansion about the epoch 2017.02, which is the mid-point of the 3-year data window. The Gauss coefficients and Euler angles were computed via a least-squares minimization of the residuals between the data and model. We used a Levenberg-Marquardt nonlinear least squares algorithm, which is described in more detail in Alken *et al.*, 2015. In order to constrain the higher degree SV and SA parameters, we regularized the model by minimizing $\langle \left| \frac{dB_r}{dt} \right|^2 \rangle$ and $\langle \left| \frac{d^2 B_r}{dt^2} \right|^2 \rangle$ averaged over the core-mantle boundary.

Once the Gauss coefficients were determined, we linearly extrapolated them back to the epoch 2015.0 using only the main field and secular variation terms (secular acceleration was ignored for the extrapolation). This procedure ensures that the model SV at 2015.0 matches the SV computed at 2017.02 (i.e. the SV error would then be lowest at epoch 2017.02) for the components which are linear functions of the Gauss coefficients, namely X, Y and Z.

b. BGS Parent Model

i. Data selection

Magnetic field measurements from the Ørsted, Swarm A, B and C satellites, and from 160 geomagnetic observatories worldwide were used. A more complete description of these data sources is given in the WMM2015-TR. Measurements span the period 2013.0 to 2018.5, as available in August 2018. Only scalar data are available from Ørsted, and only in the first half of

2013. Satellite data are 1 Hz measurements, subsampled at 20-second intervals, observatory data are hourly mean values. Both vector and scalar satellite instrument data were used from all latitudes, with scalar data only used when a concurrent vector measurement was not available. The design of the selection procedure follows that described in detail by Thomson *et al.*, 2010.

Satellite data were further refined to represent quiet, night-time behavior of the geomagnetic field using the following criteria:

- $Kp \leq 2_o$
- $|dD_{st}/dt| \leq 2$ nT/hour
- $-10 \leq IMF\ B_x \leq 10$ nT
- $-3 \leq IMF\ B_y \leq 3$ nT
- $0 \leq IMF\ B_z \leq 6$ nT
- $v_{sw} \leq 450$ km/s
- $23{:}00 \leq$ local time $\leq 05{:}00$, for geomagnetic latitudes $\leq |55°|$

Descriptions and sources of the indices Kp and Dst, and the measurements IMF B and v_{sw} are given in §2.2.3 of the WMM2015-TR.

Satellite measurements were also rejected if they represented outliers in differences to an *a priori* model (>|500| nT) or between concurrent readings from the vector and scalar instruments (>|2| nT).

Vector observatory data from geomagnetic latitudes $\leq |55°|$ were used directly, while for geomagnetic latitudes $>|55°|$ the vector measurements were projected onto an *a priori* field vector estimate to give pseudo-scalar values.

Observatory data were also further refined to represent quiet, night-time behavior of the geomagnetic field using the following criteria:

- $Kp \leq 2_+$
- $|dD_{st}/dt| \leq 5$ nT/hour
- $-2 \leq IMF\ B_z$ nT
- $01{:}00 \leq$ local time $\leq 02{:}00$

ii. Data weighting

All measurements were given prior weightings (in the form of a diagonal covariance matrix) to represent associated uncertainty and noise, based on a combination of factors, described in more detail by Lesur *et al.*, 2005,

Thomson *et al.*, 2010 and Hamilton *et al.*, 2015. For satellite data, these factors were:

- Local-scale geomagnetic activity estimate given by along-track standard deviation over each 20-second subsampling period
- Regional-scale geomagnetic activity estimate from the nearest geomagnetic observatories (Local Area Vector Activity (LAVA) index, Thomson *et al.*, 2010)
- Function of solar zenith angle (z), $2(1 + \cos z)^2$ nT
- Spatially uniform noise of 2 nT standard deviation

These factors were subsequently scaled by data density across a 1° equal-area tesseral grid.

For observatory data, weight factors were:

- Spatially uniform noise of 2 nT standard deviation, for geomagnetic latitudes ≤|55°|
- Spatially uniform noise of 6 nT standard deviation, for geomagnetic latitudes >|55°|
- Function of solar zenith angle (z), $2(1 + \cos z)^2$ nT

The values of all observatory data weights were subsequently scaled so that their total weight (sum of variances) is approximately 10% that of the total satellite data weight, in order to balance the spatial densities of observatory and satellite data sets.

iii. Model description

The parent model comprised a co-estimation of the following parameterized components (based on the detailed model description and algorithm given by Hamilton *et al.*, 2015):

- Core field: order 6 B-spline time dependence up to spherical harmonic degree 15, with 6-month spaced knots spanning 2013.0 to 2019.0, regularized by minimizing the time integral of the 3rd time derivative of the radial magnetic field over the core-mantle boundary, and the 2nd time derivative of the radial magnetic field over the core-mantle boundary at the end knots
- Crustal field: static in time and described from degree 16 to 55
- External fields: a slow time-varying external magnetospheric field of order 2 B-spline time dependence up to degree 1, using the same knots as the core field; a rapid time varying external and induced magnetospheric field scaled by the Vector Magnetic Disturbance

(VMD) index (Thomson and Lesur, 2007) with order 2 B-spline dependence up to degree 1, over 3-month spaced knots spanning 2013.0 to 2019.0; periodic terms accounting for annual, semi-annual and diurnal variations

- Crustal biases: offsets, static in time, for each observatory component

The BGS candidate model secular variation coefficients were calculated as the mean of parent model secular variation coefficients at 0.1 year intervals from 2017.0 to 2018.0, inclusive. This secular variation was then used to extrapolate the main field of the parent model at 2017.5 back to 2015.0. This process ensures a constant rate of secular variation that is representative through the 2015.0 to 2018.5 period covered by our data set, with a main field valid at 2015.0 but most accurate at 2017.5.

c. Validation process and combining both models into the final WMM2015v2

Each parent model was validated by comparing it to other similar recent models and to a global set of geomagnetic observatory data. In particular, we checked that both parent models had smaller secular variation errors in 2017.5 than in 2015.0, as intended (see section 3). Inter-comparison of NOAA/NCEI and BGS parent models also provided a semi-independent validation of each model, as both models were derived using slightly different datasets and methods, and fully independent algorithms.

After both parent models were validated, the main field and secular variation coefficients were truncated to spherical harmonic degree and order 12 for both models. Then, the final model coefficients were computed as averages between the two sets of coefficients from the two parent models. The final model was again validated using the approach discussed above before being approved for public release.

3. Model Uncertainties

The WMM provides a mathematical description of the main field and its secular variation up to spherical harmonic degree and order 12. WMM uncertainties are of two types: the commission error, which is caused by inaccuracies in model coefficients, and the omission error, which is due to un-modeled contributions to the total magnetic field, e.g., magnetic fields of spatial scales smaller than the smallest WMM scale (about 3000 km at the equator) or rapid magnetic field variations that cannot be represented by a linear function over five years. A description of the various sources of uncertainty and their contributions to the overall WMM error budget may be found in the WMM2015-TR.

Of special interest here is the secular variation error, which falls under both the commission and the omission error types. By definition, each WMM is calculated from data collected prior to the WMM validity interval. For example, the WMM2015 was derived from satellite data spanning the time intervals 2013.0 to 2014.8 (main field) and 2009.0 to 2014.8 (secular variation). As a result, even though the WMM secular variation is accurate at the beginning of the five-year interval (e.g., in 2015.0), it generally becomes less accurate as time advances due to changes in the actual secular variation. Such changes are difficult to predict and are caused by the "secular acceleration", i.e., the second order time derivative of the magnetic field of internal origin, which is not included in the WMM. In that sense, the associated error is an omission type of error. It generally becomes larger as time passes.

Figure 1 shows the root-mean-square (RMS) error in the grid variation (GV) component of the magnetic field over the WMM2015 time interval. As GV and declination differ by only a constant (see WMM2015-TR), the GV error is the same as the declination error over polar areas (above 55 / below -55 degrees latitudes). The total RMS GV error was obtained as follows:

a) take the average of the declination values in Table 14, rows 4 and 5 (obtained using two different methods) of the WMM2015-TR to obtain the average crustal field and secular variation declination error at all latitudes (result: 0.38 degree);

b) remove (in an RMS sense) the average secular variation contribution, calculated by comparing WMM and retrospective models over 15 years, to obtain an estimate of the crustal field only declination error (result: 0.37 degree);

c) assuming the crustal field error is the same all over the globe, including in the polar regions, add (in an RMS sense) the crustal field declination error (0.37 degree) to the average disturbance field GV error (0.52 degree) found in Table 14, row 6 of the WMM2015-TR to obtain the total omission GV error (result: 0.64 degree);

d) add (in an RMS sense) the omission GV error to the time-varying secular variation error, estimated by comparing the WMM2015 GV with GV calculated from more recent geomagnetic field models including data until mid-2018.

These calculations were done by NOAA/NCEI. GV is not defined at the exact poles and different results are obtained depending on sampling of the surface. BGS therefore obtained slightly different results. A future version of the military specification may alleviate these ambiguities.

As can be seen in Figure 1, the GV error regularly increased after 2015.0, due to the cumulative effect of small changes in the actual secular variation. Although an increase in error over time is also observed in other components (not shown here), this effect is largest for GV, due to the geometry of the magnetic field near the poles. Assuming no secular acceleration after 2018, we extrapolated the GV error and found that it was on a trajectory to exceed the WMM accuracy requirement of 1-degree RMS error for GV at the end of 2018.

The WMM2015v2 significantly reduces the secular variation error over the entire 2015-2020 interval, as shown in Figure 1. The main reason for this improvement is that WMM2015v2 includes more recent data, thus allowing for a more accurate determination of the average secular variation over the entire interval. As the WMM2015v2 parent models are either centered around 2017.02 or designed to provide the most accurate main field at 2017.5 (see section 2), the GV error is minimum in the first half of year 2017; it is maximum at both ends of the 2015-2020 interval due to the cumulative effect of the secular variation error. However, even at 2015.0 and 2020.0, the error remains well below the WMM performance requirement for GV.

The RMS GV error shown in Figure 1 is the sum of the errors in both polar caps. The RMS GV error in the Northern polar cap (GVN, Figure 2) increased much faster than the error in the Southern polar cap (GVS, not shown), due to the larger secular variation in the North. The GVN error exceeded the 1-degree specification as early as early-2018, whereas the GVS error is well below the specification and is not expected to exceed it by the end of the 2015.0—2020.0 time interval. The WMM2015 performance degradation is only an issue in the Northern polar cap.
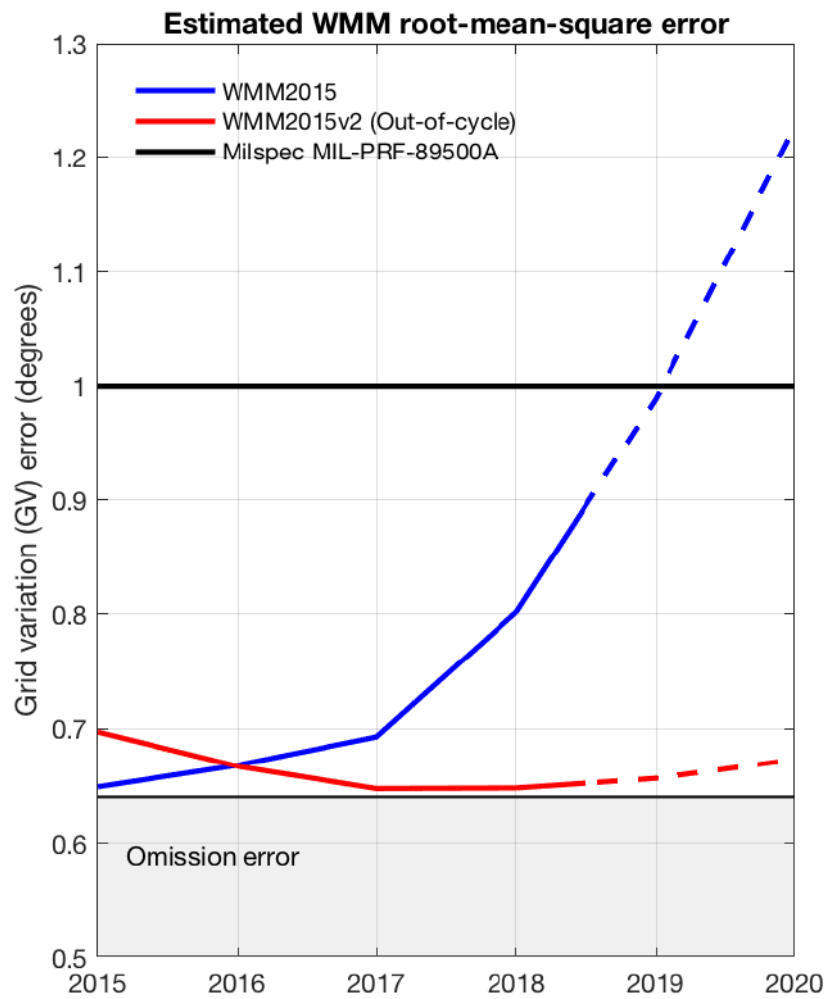
Figure 1: RMS GV (Grid Variation North and South) error as a function of time, WMM2015 and WMM2015v2 models.
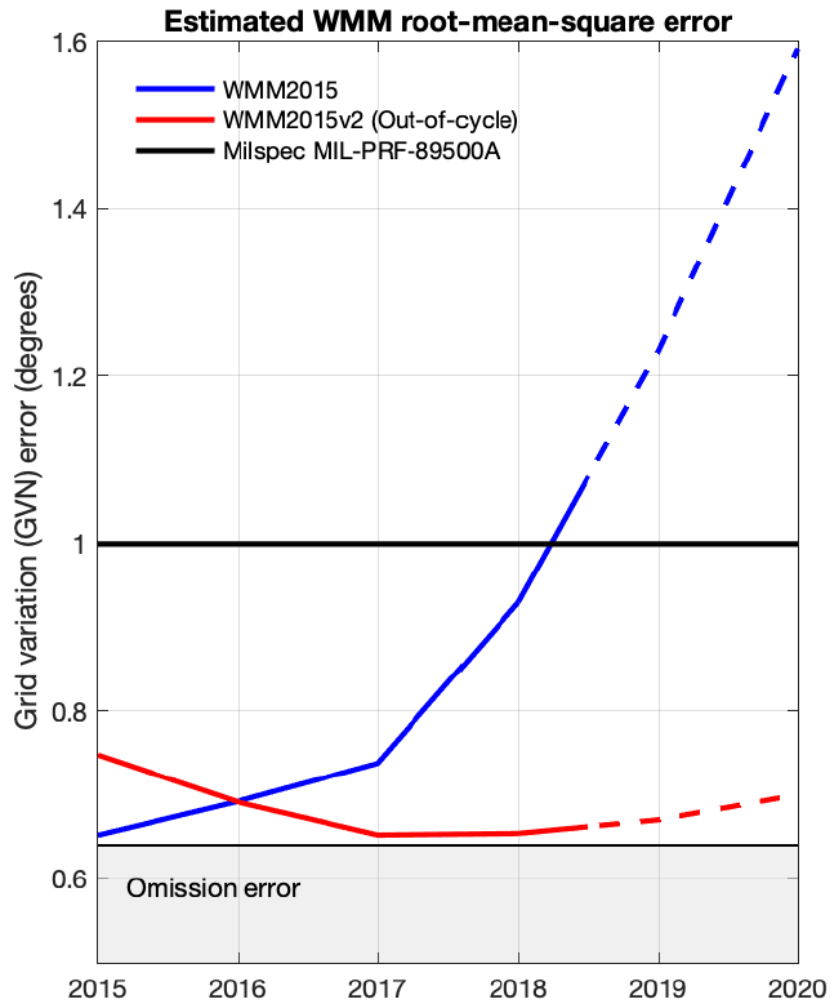
Figure 2: RMS GVN (Grid Variation North) error as a function of time, WMM2015 and WMM2015v2 models.

4. Charts

All the charts provided in the WMM2015-TR were updated using WMM2015v2. For example, Figure 3 shows the main field declination in the north polar region. Charts and corresponding shapefiles are available from
https://www.ngdc.noaa.gov/geomag/WMM/data/WMM2015/WMMMaps2015v2.zip,
ftp://ftp.ngdc.noaa.gov/geomag/wmm/wmm2015v2/shapefiles/.
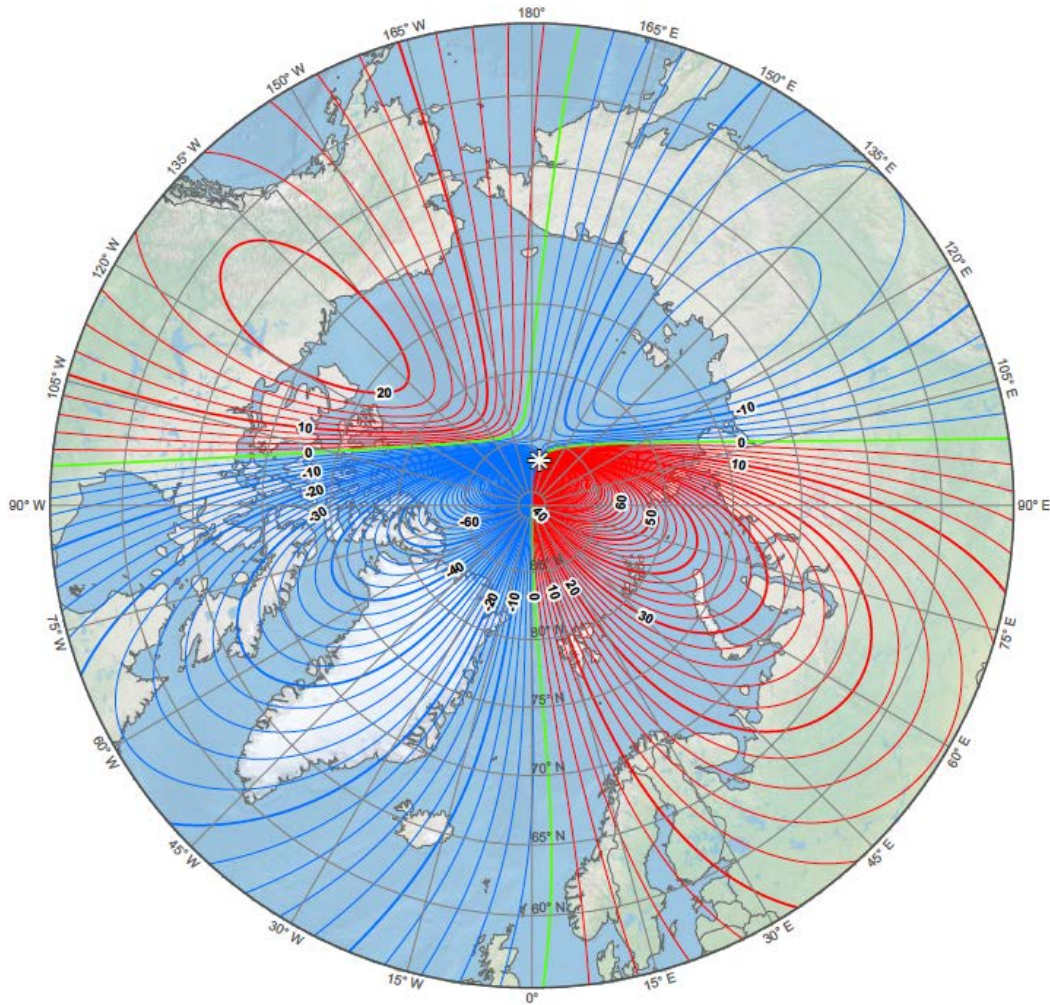
Figure 3: Main field declination (D) at 2019.0 from WMM2015v2. Contour interval is 2 degrees, red contours positive (east); blue negative (west); green zero (agonic) line. North polar region. Polar Stereographic Projection. The white star indicates the 2019.0 position of the dip pole.

References and Bibliography

Alken, P., S. Maus, A. Chulliat and C. Manoj, NOAA/NGDC Candidate Models for the 12th generation International Geomagnetic Reference Field, Earth Planets Space, 67:68, 2015, doi: 10.1186/s40623-015-0215-1.

Chulliat, A., S. Macmillan, P. Alken, C. Beggan, M. Nair, B. Hamilton, A. Woods, V. Ridley, S. Maus and A. Thomson, The US/UK World Magnetic Model for 2015--2020: Technical Report, National Geophysical Data Center, NOAA, 2015, doi: 10.7289/V5TB14V7.

Lesur, V., S. Macmillan and A. Thomson, The BGS magnetic field candidate models for the 10th generation IGRF. Earth, Planets and Space, 57(12), 1157-1163, 2005, doi: 10.1186/BF03351899.

Hamilton, B., V. A. Ridley, C. D. Beggan and S. Macmillan, The BGS magnetic field candidate models for the 12th generation IGRF. Earth, Planets and Space, 67(1), 2015, doi: 10.1186/s40623-015-0227-x.

Lühr, H. and S. Maus, Solar cycle dependence of quiet-time magnetospheric currents and a model of their near-Earth magnetic fields. Earth, Planets and Space, 62(10), p.14, 2010, doi: 10.5047/eps.2010.07.012.

MIL-PRF-89500A, Performance Specification, World Magnetic Model (WMM), Department of Defense, 30 October 2015.

Olsen, N., H. Lühr, C.C. Finlay, T.J. Sabaka, I. Michaelis, J. Rauberg and L. Tøffner-Clausen, The CHAOS-4 geomagnetic field model. Geophysical Journal International, 197(2), 815-827, 2014, doi: 10.1093/gji/ggu033.

Thomson, A. W. P. and V. Lesur, An Improved Geomagnetic Data Selection Algorithm for Global Geomagnetic Field Modelling. Geophysical Journal International, 169(3), 951-963, 2007, doi: 10.1111/j.1365-246X.2007.03354.x.

Thomson, A. W. P., B. Hamilton, S. Macmillan and S. J. Reay, A novel weighting method for satellite magnetic data and a new global magnetic field model. Geophysical Journal International, 181(1), 250-260, 2010, doi: 10.1111/j.1365-246X.2010.04510.x.